Universal Density of States for Carbon Nanotubes

J. W. Mintmire and C. T. White
Code 6179, U.S. Naval Research Laboratory, Washington, D.C. 20375-5342
(Received 13 March 1998)

The density of states in the vicinity of the Fermi level of single-wall carbon nanotubes can be expressed in terms of a universal relationship that depends only on whether the nanotube is metallic or semiconducting. We compare the predictions of this approximate relationship with densities of states calculated using first-principles band structure results. These comparisons show that this approximation works well for energies within about 1 eV of the Fermi level. [S0031-9007(98)07132-4]

PACS numbers: 71.20.Tx, 71.15.Fv, 71.15.Mb, 73.61.Wp

Scanning tunneling microscopy (STM) and spectroscopy experiments have been recently reported for individual single-wall carbon nanotubes (SWNT) [1,2], confirming the strongly one-dimensional nature expected for the electron states in these materials [3,4]. The STM experiments give a direct experimental probe of the electron density of states (DOS) near the Fermi level. We have recently shown that semiconducting SWNTs with similar diameters will have similar DOS near the Fermi level, and established an analogous correspondence for metallic nanotubes [5]. We also gave expressions for the positions of the peaks near the Fermi level. Here we derive a universal relationship for the DOS in the vicinity of the Fermi level for SWNTs. This relationship, based on the graphene sheet model, scales out the dependence on the nanotube diameter and otherwise only depends on whether the SWNT belongs to the semiconducting or metallic groups of nanotubes. We compare the predictions of this relationship with the DOS results calculated using first-principles band structure results for SWNTs with diameters ranging from 1.3 to 2.8 nm.

A SWNT can be constructed by rolling up a single graphene sheet (depicted in Fig. 1) along one of its 2D lattice vectors $\mathbf{R} = n_1\mathbf{R}_1 + n_2\mathbf{R}_2$ to form a (n_1, n_2) nanotube with radius $r = |\mathbf{R}|/2\pi$. Perhaps the simplest model for the electronic structure of SWNTs is a Slater-Koster or Hückel tight-binding model of the graphene sheet with periodic boundary conditions imposed over the rollup vector $\mathbf{R}$. The Brillouin zone of graphene is hexagonal as depicted in Fig. 2, with reciprocal lattice vectors $\mathbf{K}_1$ and $\mathbf{K}_2$ defined in terms of the real lattice vectors by the relationship $\mathbf{K}_i \cdot \mathbf{R}_j = 2\pi\delta_{ij}$. The Fermi level for graphene occurs at the vertices of the hexagons at the points k_F located by the vectors $\mathbf{K}_F \equiv \pm(\mathbf{K}_1 - \mathbf{K}_2)/3$, $\pm(2\mathbf{K}_1 + \mathbf{K}_2)/3$, and $\pm(\mathbf{K}_1 + 2\mathbf{K}_2)/3$. Allowed electron states for the nanotube are then restricted to points k, located by the two-dimensional wave vector $\mathbf{k}$, which satisfy the boundary condition $\mathbf{k} \cdot \mathbf{R} = 2\pi m$, corresponding to the parallel lines in Fig. 2. This approach has been used to group the SWNTs into metallic and semiconducting nanotubes depending on whether $n_1 - n_2$ is an integer multiple of 3 (metallic) or not (semiconducting) [6–11]. With curvature effects included, group symmetry can be used to show that only the armchair SWNTs ($n_1 = n_2$ and the symmetry equivalent SWNTs $n_1 = -2n_2$ and $n_2 = -2n_1$) are truly metallic [6]; all other SWNTs satisfying the metallic condition are only quasimetallic with small band gaps varying as the inverse square of the SWNT radius [12,13].

In general, the contribution of a single, doubly degenerate 1D band $\varepsilon(k)$ to the density of states, $n(E) = \partial N(E)/\partial E$, can be expressed as

$$n(E) = \frac{2}{\ell} \sum_i \int dk\, \delta(k - k_i) \left| \frac{\partial \varepsilon}{\partial k} \right|^{-1}, \qquad (1)$$

where k_i are the roots of the equation $E - \varepsilon(k_i) = 0$, ℓ is the length of the 1D Brillouin zone $\ell = \int dk$, and $N(E)$ is the total number of electron states per unit cell below a given energy E. Because the hexagonal Brillouin zone depicted in Fig. 2 tiles the entire two-dimensional plane, the total area of the graphene central Brillouin zone must equal the product of the total length of the allowed state lines in the Brillouin zone times the

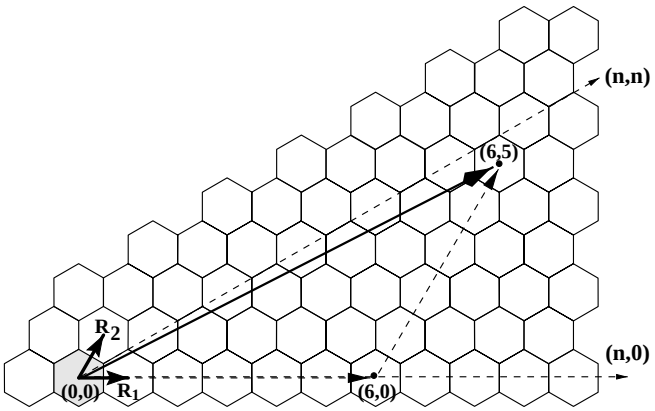

FIG. 1. Two-dimensional graphene lattice structure. Primitive lattice vectors $\mathbf{R}_1$ and $\mathbf{R}_2$ are depicted in origin unit cell. Rollup vector $\mathbf{R}$ is shown for (6, 5) SWNT. Armchair nanotubes are defined by rollup vectors along the (n, n) direction, zigzag nanotubes are defined by rollup vectors along the $(n, 0)$ direction. Armchair and zigzag nanotubes will possess reflection planes and be achiral, all other SWNTs will be chiral.

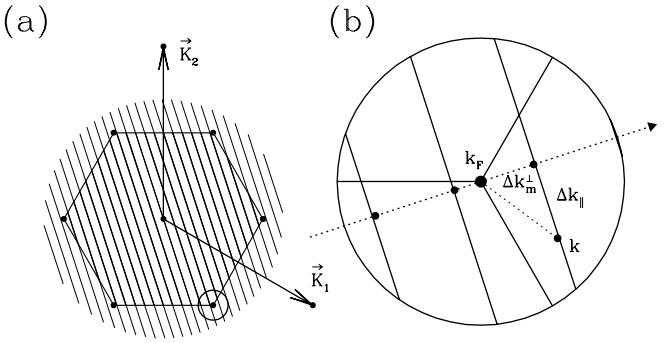

FIG. 2. (a) Hexagonal central Brillouin zone of graphene. Parallel lines depict allowed states for (13, 6) SWNT. Circle at bottom right encloses the region of states near ε_F. Lines with arrows denote reciprocal lattice vectors $\mathbf{K}_1$ and $\mathbf{K}_2$. (b) Expanded depiction of allowed states near ε_F, with dotted line parallel to $\mathbf{R}$ and the k_F corner of hexagon with energy ε_F. $\mathbf{k}$ denotes the arbitrary point on the allowed state line near $\mathbf{k}_F$, with $\Delta k_m^\perp$ and $\Delta k_\parallel$ the components perpendicular and parallel, respectively, to the allowed state lines.

spacing between lines. For the nanotube states defined by the graphene sheet model, this total length ℓ will thus equal the total area of the Brillouin zone, $\Omega_{\mathrm{BZ}} = 8\pi^2/(a^2\sqrt{3})$, where a is the graphene lattice spacing $a = |\mathbf{R}_1| = |\mathbf{R}_2|$ divided by the interline spacing $2\pi/|\mathbf{R}|$, or $\ell = (4\pi/\sqrt{3})|\mathbf{R}|/a^2$. This corresponds to a normalization over the graphene sheet unit cell, or the DOS per every two carbons.

The DOS near the Fermi level will be directly related to the energy levels of the states near the corners of the Brillouin zone, k_F. Near ε_F, the 2D dispersion relations of the occupied and unoccupied π bands of graphene using a nearest-neighbor interaction $V_{pp\pi}$ are given to good approximation [for $|\varepsilon(\mathbf{k})/V_{pp\pi}| \ll 1$] by [11]

$$|\varepsilon(\mathbf{k})| \approx (\sqrt{3}/2)a|V_{pp\pi}||\mathbf{k} - \mathbf{k}_F|, \tag{2}$$

and are radially symmetric around the point k_F. Using this approximation, we can construct the DOS of the carbon nanotube in the vicinity of ε_F. Over the region where Eq. (2) is valid, the point of closest approach to k_F in any line near k_F (but not intersecting) will represent a local maximum (minimum) in the 1D band structure, leading to a van Hove singularity and a divergence in the occupied (unoccupied) DOS near ε_F [5]. The length of the vector $\mathbf{k} - \mathbf{k}_F$, between k_F and one of the allowed states at k satisfying $\mathbf{k} \cdot \mathbf{R} = 2\pi m$, will be given by $|\mathbf{k} - \mathbf{k}_F|^2 = \Delta k_m^{\perp 2} + \Delta k_\parallel^2$, where $\Delta k_m^\perp$ and $\Delta k_\parallel$ denote the perpendicular and parallel (with respect to the allowed state lines) components, respectively, of $\mathbf{k} - \mathbf{k}_F$ as depicted in Fig. 2a. The perpendicular component $\Delta k_m^\perp$ is quantized and given by [5]

$$\Delta k_m^\perp = \left| (\mathbf{k} - \mathbf{k}_F) \cdot \frac{\mathbf{R}}{|\mathbf{R}|} \right| = \frac{2\pi}{3|\mathbf{R}|}|3m - n_1 + n_2|. \tag{3}$$

The contribution of the state at k to the DOS [at energy $\varepsilon(\mathbf{k})$ in the graphene Brillouin zone] using Eq. (1) will be given by

$$\left| \frac{\partial \varepsilon}{\partial k_\parallel} \right|^{-1} = \frac{2}{\sqrt{3}\,|V_{pp\pi}|a} \frac{|\varepsilon|}{\sqrt{\varepsilon^2 - \varepsilon_m^2}}, \tag{4}$$

where, from Eqs. (2) and (3),

$$|\varepsilon_m| = \frac{\sqrt{3}}{2}|V_{pp\pi}|a\Delta k_m^\perp = \frac{|3m - n_1 + n_2|}{2}|V_{pp\pi}|\frac{d}{r}, \tag{5}$$

with d the carbon-carbon bond distance ($a = d\sqrt{3}$) and r is the nanotube radius ($|\mathbf{R}| = 2\pi r$).

Before applying Eq. (4) to Eq. (1), each line in the vicinity of k_F at $\mathbf{k}_F$ will have two points at any given energy $\varepsilon(\mathbf{k})$, and, in addition to these two points two more equivalent points in the vicinity of the point located by $-\mathbf{k}_F$ will contribute to the DOS at this energy. In all, we can then write the DOS per carbon atom, $\rho(E) = n(E)/2$, as

$$\begin{aligned}\rho(E) &= \frac{4}{\ell}\sum_{m=-\infty}^{\infty}\frac{2}{\sqrt{3}\,|V_{pp\pi}|a}\,g(E,\varepsilon_m) \\ &= \frac{\sqrt{3}}{\pi^2}\frac{1}{|V_{pp\pi}|}\frac{d}{r}\sum_{m=-\infty}^{\infty}g(E,\varepsilon_m),\end{aligned} \tag{6}$$

where

$$g(E,\varepsilon_m) = \begin{cases} |E|/\sqrt{E^2 - \varepsilon_m^2}, & |E| > |\varepsilon_m|; \\ 0, & |E| < |\varepsilon_m|. \end{cases} \tag{7}$$

We note that $g(E,\varepsilon_m)$ exhibits a divergent van Hove singularity at $|E| = |\varepsilon_m|$ for $|\varepsilon_m| \neq 0$, and that $g(E,0) = 1$.

The DOS in the vicinity of the Fermi level of all carbon nanotubes can then be expressed in terms of a universal function $U(E')$:

$$\rho(E) = \frac{1}{\Lambda|V_{pp\pi}|}\,U\!\left(\frac{\Lambda E}{|V_{pp\pi}|}\right), \tag{8}$$

where Λ is the dimensionless ratio of the nanotube diameter to the carbon-carbon bond distance, $\Lambda = 2r/d = \sqrt{3(n_1^2 + n_2^2 + n_1 n_2)}/2\pi$, and $U(E')$ is given by

$$U(E') = \frac{2\sqrt{3}}{\pi^2}\sum_{m'=-\infty}^{\infty}g(E',\varepsilon'_{m'}), \tag{9}$$

with $|\varepsilon'_{m'}|^2 = (3m' + 1)^2$ for semiconducting ($n_1 - n_2 \neq 3q$) and $|\varepsilon'_{m'}|^2 = (3m')^2$ for metallic ($n_1 - n_2 = 3q$) tubes with q an integer. In terms of the scaled energy $E' = \Lambda E/|V_{pp\pi}|$, Eq. (2) used to derive Eq. (9) will be valid for $|E'| \ll \Lambda$. Recent experimental STM results have been reported for SWNTs with diameters of roughly 1.4 nm compared to a carbon-carbon bond distance in graphite of 0.14 nm, and a corresponding ratio of $\Lambda \approx 10$ [1,2].

To test the applicability and universality of Eq. (9)—obtained by approximating $\varepsilon(\mathbf{k}_F)$ by Eq. (2) and negelecting the effects of curvature—we have carried

out first-principles local-density functional band structure calculations for several SWNTs with diameters ranging from 1.28 to 2.82 nm. All calculations were performed on SWNTs using a carbon-carbon bond distance of $d = 0.144$ nm that was found to optimize the geometry of the (5, 5) SWNT [14], using methods that have been described in detail elsewhere [15,16]. For the first-principles results, we started by numerically calculating the DOS from the one-electron bands per carbon atom and scaled these results by the appropriate value of Λ and an effective value of $|V_{pp\pi}|$ of 2.5 eV.

In Fig. 3 we depict our calculated first-principles DOS for the (16, 0), (13, 6), and (21, 20) SWNTs (with diameters of 1.28, 1.34, and 2.82 nm, respectively) versus the universal function $U(E')$. These first-principles results are both in good agreement with the universal relationship and with each other for a range of roughly $|E'| < 3 \ll \Lambda$. A theoretical DOS of a (16, 0) nanotube was used by Wildöer, *et al.* [1] in a comparison with experimental STM measurements of the DOS of a 1.3 nm diameter SWNT. The low-energy DOS of the similar diameter chiral (13, 6) SWNT is essentially the same as that of the achiral (16, 0) SWNT, consistent with our earlier analysis [5]. Figure 3 demonstrates that the scaled low-energy DOS for these 1.3 nm diameter nanotubes will also be similar to the scaled DOS for the 2.8 nm (21, 20) nanotube and other semiconducting SWNTs over a range of diameters.

Similarly, in Fig. 4 we compare our first-principles results for the (10, 10), (14, 5), and (22, 19) SWNTs (with diameters of 1.38, 1.36, and 2.82 nm, respectively) with the universal relationship. Our sample set of metallic SWNTs thus represents the (10, 10) SWNT observed by Thess, *et al.* [17], a similar diameter chiral (14, 5) SWNT, and a (22, 19) chiral SWNT with twice the diameter of the previous two nanotubes. The (10, 10) nanotube is an achiral armchair nanotube, which exhibits a metallic band structure even at the first-principles level [6]. The (14, 5) and (22, 19) nanotubes will only be quasimetallic, with a band gap introduced at the Fermi level by curvature effects, with calculated band gaps of 0.03 and 0.001 eV, respectively. This gap shows up as the two relatively small peaks immediately around the Fermi level, which might be observable as weak broadened features in experiments. The initial principal peaks near the Fermi level will occur at an energy three times that in the semiconducting SWNTs [5], and this peak essentially represents the limit of agreement between the first-principles results and the universal relationship for tubes with diameters of about 1.4 nm. The occupied DOS in the first-principles results are all better described by the universal relationship than are the unoccupied DOS results. For the armchair nanotubes the DOS will have two identical contributions, one from each sign of the pair of values $\pm\varepsilon_m \neq 0$. For other quasimetallic nanotubes this degeneracy is broken because of deviations of the true dispersion energy $\varepsilon(\mathbf{k})$ from radial symmetry at about k_F. In the first-principles results, the DOS at $E' \approx \pm 3$ have two inequivalent van Hove singularities for the quasimetallic (15, 0) and (13, 7) nanotubes, which might allow armchair nanotubes to be differentiated from other quasimetallic nanotubes with sufficiently resolved experiments.

In summary, we have derived a universal relationship for the low-energy DOS for carbon nanotubes. We have shown that for energies $|\varepsilon - \varepsilon_F| \ll |V_{pp\pi}|$ the DOS line

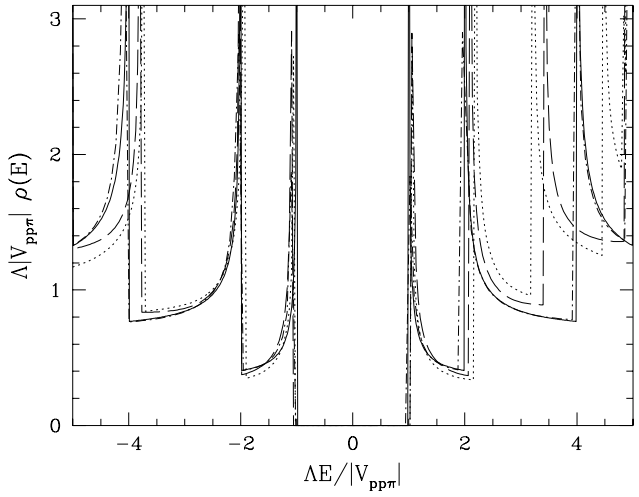

FIG. 3. Comparison of scaled first-principles DOS results with universal relationship from Eq. (9). Solid line depicts results for the universal relationship for semiconducting nanotubes ($n_1 - n_2 \neq 3q$), dotted line depicts scaled first-principles band structure results for (16, 0) SWNT, dashed line depicts results for (13, 6) SWNT, and dot-dashed line depicts results for (21, 20) SWNT.

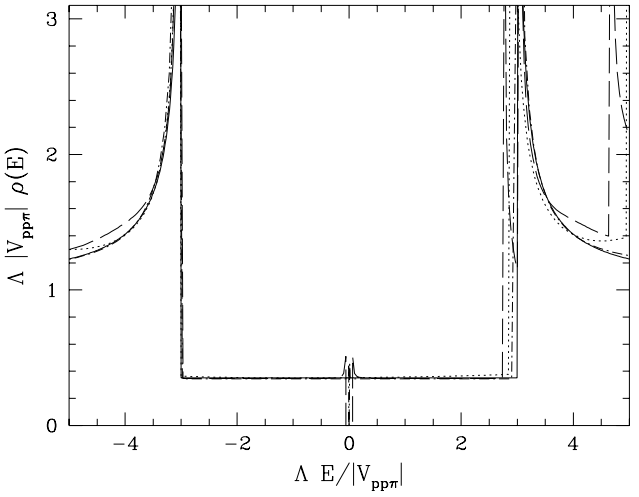

FIG. 4. Comparison of scaled first-principles DOS results with universal relationship from Eq. (9). The solid line depicts results for a universal relationship for metallic nanotubes ($n_1 - n_2 = 3q$), dotted line depicts scaled first-principles band structure results for (10, 10) SWNT, dashed line depicts results for (14, 5) SWNT, and dot-dashed line depicts results for (22, 19) SWNT.

shapes for all semiconducting nanotubes can be reduced by appropriate scaling to the same function, and all metallic nanotubes can be reduced to a related function. Comparison with first-principles DOS suggest that this model should be valid over a region several eV's wide. In addition to the obvious implications of this work on experimental measurements of the DOS of SWNTs of differing diameters, this universal relationship should be important in understanding a range of spectroscopic and other experimental measurements which are dependent on the DOS near the Fermi level.

This work was supported by the U.S. Office of Naval Research, both directly and through the Naval Research Laboratory. A grant of computational time was provided under the DOD High Performance Computing Initiative Program.

[1] J. W. G. Wildöer, L. C. Venema, A. G. Rinzler, R. E. Smalley, and C. Dekker, Nature (London) **391**, 59 (1998).
[2] T. W. Odom, J.-L. Huang, P. Kim, and C. M. Lieber, Nature (London) **391**, 62 (1998).
[3] *Carbon Nanotubes: Preparation and Properties*, edited by T. W. Ebbesen (CRC, Boca Raton, 1997), and references therein.
[4] M. S. Dresselhaus, G. Dresselhaus, P. C. Eklund, *Science of Fullerenes and Carbon Nanotubes* (Academic, San Diego, 1996).
[5] C. T. White and J. W. Mintmire, Nature (London) **394**, 29 (1998).
[6] J. W. Mintmire, B. I. Dunlap, and C. T. White, Phys. Rev. Lett. **68**, 631 (1992).
[7] J. W. Mintmire, D. H. Robertson, B. I. Dunlap, R. C. Mowrey, D. W. Brenner, and C. T. White, in *Electrical, Optical, and Magnetic Properties of Organic Solid State Materials*, edited by L. Y. Chiang, A. F. Garito, and D. J. Sandman, MRS Symposia Proceedings No. 247 (Materials Research Society, Pittsburgh, 1992), p. 339.
[8] N. Hamada, S. Sawada, and A. Oshiyama, Phys. Rev. Lett. **68**, 1579 (1992).
[9] R. Saito, M. Fujita, G. Dresselhaus, and M. S. Dresselhaus, Phys. Rev. B **46**, 1804 (1992); Appl. Phys. Lett. **60**, 2204 (1992).
[10] C. T. White, D. H. Robertson, and J. W. Mintmire, Phys. Rev. B **47**, 5485 (1993).
[11] J. W. Mintmire, D. H. Robertson, and C. T. White, J. Phys. Chem. Solids **54**, 1835 (1993).
[12] C. T. White, D. H. Robertson, and J. W. Mintmire, in *Clusters and Nanostructured Materials*, edited by P. Jena and S. Behera (Nova, New York, 1996), p. 231.
[13] C. L. Kane and E. J. Mele, Phys. Rev. Lett. **78**, 1932 (1997).
[14] D. H. Robertson, D. W. Brenner, and J. W. Mintmire, Phys. Rev. B **45**, 12 592 (1992).
[15] J. W. Mintmire and C. T. White, Phys. Rev. Lett. **50**, 101 (1983); Phys. Rev. B **28**, 3283 (1983).
[16] J. W. Mintmire, in *Density Functional Methods in Chemistry*, edited by J. Labanowski and J. Andzelm (Springer-Verlag, New York, 1991), pp. 125–138.
[17] A. Thess, R. Lee, P. Nikolaev, H. Dai, P. Petit, J. Robert, C. Xu, Y. H. Lee, S. G. Kim, A. G. Rinzler, D. T. Colbert, G. E. Scuseria, D. Tománek, J. E. Fischer, and R. E. Smalley, Science **273**, 483 (1996).